geoconvention
Virtual Event
September 21-23
2020
CSPG • CSEG • CWLS • GAC • MAC • IAH

Clay minerals in black shales – an example from the Upper Devonian Duvernay Formation, Western Canada Sedimentary Basin

Nicholas B. Harris[1], Tian Dong[2,1], David L. Bish[3], Hui Li[1], Nina Zeyen[1]

[1] University of Alberta, [2] China University of Geosciences (Wuhan), [3] University of Indiana

Summary

Clay minerals represent a major component of organic-rich mudstones ('black shales') and are significant to geomechanical properties, petrophysical properties and log interpretation. In addition, clay mineral reactions, specifically the conversion of highly expandable smectite-rich mixed-layer clay to less expandable illite-rich clay, are related to a suite of important diagenetic reactions that include dissolution of K-feldspar and precipitation of Na-feldspar, quartz, carbonate and chlorite cements. A strong temperature control on the smectite-to-illite conversion has been demonstrated in Neogene and Paleogene mudstones of the Gulf of Mexico, with the reaction taking place largely between 70° and 100°C.

We examine the clay mineralogy of the Duvernay Formation in context of current models for the mixed layer clay reaction. In contrast to Gulf of Mexico models, clays even at shallow depths, low temperatures and low thermal maturities are dominated by highly illitic mixed layer clays, and little change is seen in the clay mineral assemblage with increasing depth and temperature. We suggest that the conversion of smectitic to illitic mixed layer clay in organic-rich shales was catalyzed by microbially mediated iron reduction in the mixed layer clays, occurring at anomalously low temperatures.

Background

The conversion of smectite-rich to illite-rich mixed-layer clay is the crux of a suite of mineral reactions in mudrocks, associated with the dissolution of potassium feldspar, albitization of detrital feldspar and the formation of authigenic albite, and the formation of late-stage iron- and magnesium-rich carbonates, clays (chlorite) and quartz cement (e.g. Boles and Franks, 1979, Land et al., 1997). Control of the smectite-to-illite reaction in mudrocks has been largely attributed to elevated temperatures. Early studies of mudrocks in the Tertiary Gulf of Mexico section by Hower et al. (1976) identified a fairly narrow window between 2800 and 3300 meters in which the reaction takes place. Subsequent studies (for example, Freed and Peacor, 1989) expanded the range of temperatures over which this reaction is observed; the wider range is attributed to variation in the initial composition and petrophysical properties of the sediment.

It is an open question, however, whether Gulf of Mexico models for clay mineral reactions apply to other mudrock systems. The former are based on mudrocks that are notably silty and organic-lean in comparison to organic-rich shales that are commonly finer grained and, more important, contain abundant organic carbon. The analysis reported here is an initial effort to compare and contrast diagenesis in organic-rich mudrocks to standard models for mudrock diagenesis.

Method / Workflow

Samples were obtained from five long drill cores across the Western Canada Sedimentary Basin (WCSB (Figure 1) that represent a range of maturities from immature (Esso Redwater) to dry gas window (Encana Cecilia). The cores were previously logged for facies analysis (Knapp et al., 2017) and characterized for geomechanical and petrophysical properties (Dong et al., 2018, 2019). Samples described here were part of a larger set of geochemistry samples reported in Harris et al. (2018). Samples consisted of 10 cm long slabs cut from the back of cores that were subsequently split vertically into aliquots for multiple analyses. Estimations of thermal maturity were derived from the Tmax parameter of Rock-eval pyrolysis analysis and corroborated by bitumen reflectance (Harris et al., 2018).

X-ray diffraction samples were analyzed at the University of Indiana (IU) Department of Earth and Atmospheric Sciences under the supervision of Dr. David Bish. Samples analyzed at IU were crushed and ground into fine powder and then were analyzed by a Bruker D8 Advance X-ray diffractometer equipped with a Sol-X solid-state detector and a Cu X-ray tube. Bulk mineralogical analysis was performed on random mounts of whole-rock powders, scanned from 2-70o at a rate of approximately 0.5 degree/minute. Oriented mounts of separated clay-size fraction (< 2 μm) were scanned from 2-20° both after air drying and after exposure to ethylene glycol vapor. Rietveld refinements with Bruker AXS TOPAS software were used to determine the absolute concentrations of each mineral.

Results

Mineralogical results are summarized in Table 2. In terms of bulk composition, West Shale Basin wells are distinguished by elevated quartz, K-feldspar and clay contents and the East Shale Basin by higher calcite content. Plagioclase and mica contents is slightly elevated in the West Shale Basin samples. The concentrations of other minor phases, including dolomite, ankerite and pyrite, are not systematically different between the two areas.

Clay contents range from 2 to 13% in East Shale Basin wells and from 0 to 37% in West Shale Basin wells and consist primarily of illite with minor chlorite (Figure 2). One sample from the lowest maturity well, the Esso Redwater, contains a highly illitic mixed-layer clay, with an expandability of approximately 5%.

Discussion

At low thermal maturities, consistent with maturation levels in the Esso Redwater core, any mixed-layer clays entering the basin should have retained their smectitic character, at least according to reaction models based on Gulf of Mexico. Thus, the presence of low expandability, highly illitic mixed-layer clay in a low thermal maturity sample and illite clay in remaining samples (Figure 2) suggests that mixed-layer smectitic clays may have never entered the basin during Duvernay deposition or, alternatively, a different model for smectite-to-illite conversion should be adopted for these rocks, either because of geologic age or because of a fundamentally different initial composition.

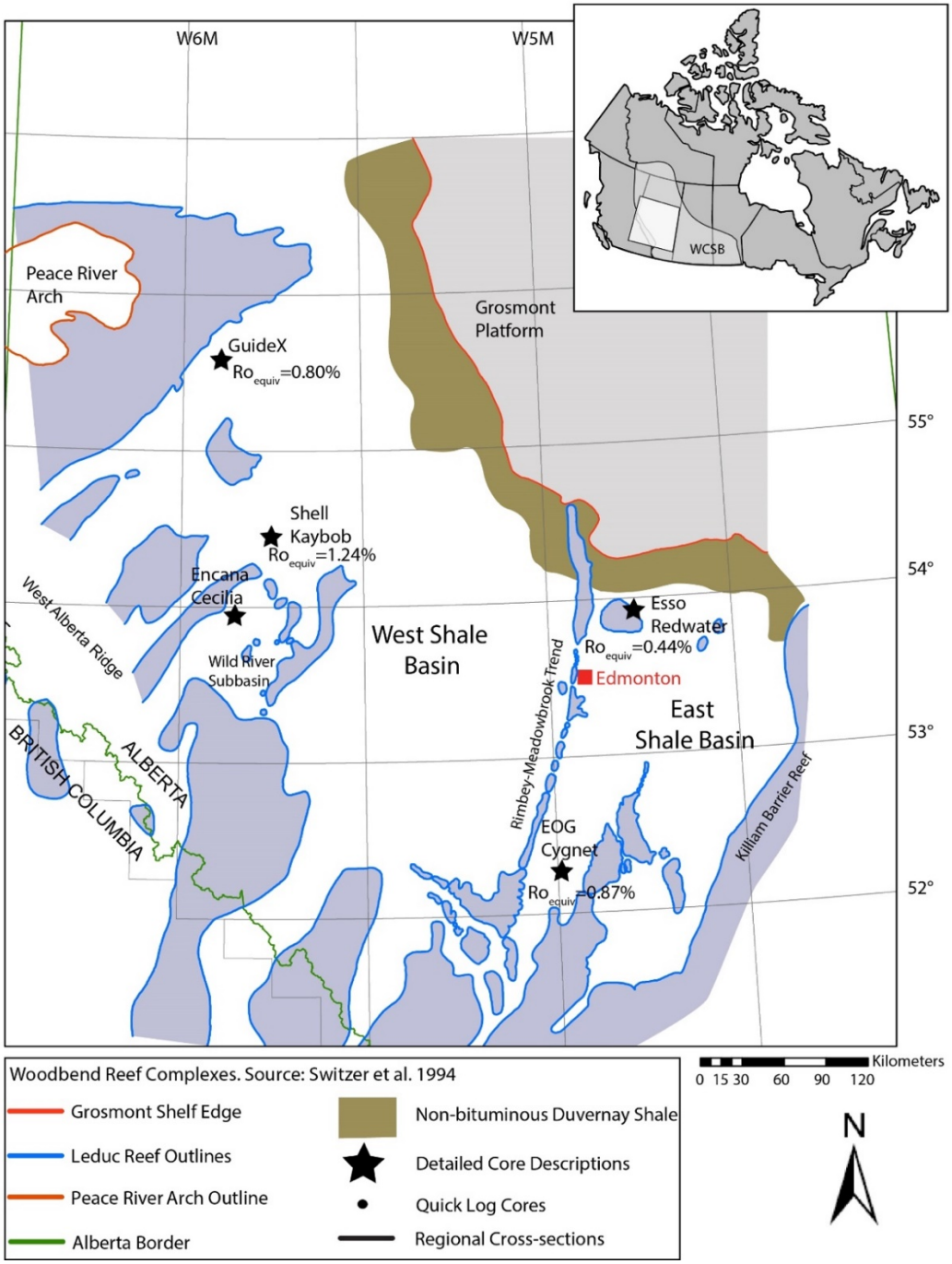

Figure 1. Location map for well discussed in this presentation, with thermal maturities calculated from Tmax data. Ro_{equiv} is calculated from an equation in Jarvie (2015). Figure modified from Harris et al. (2018).

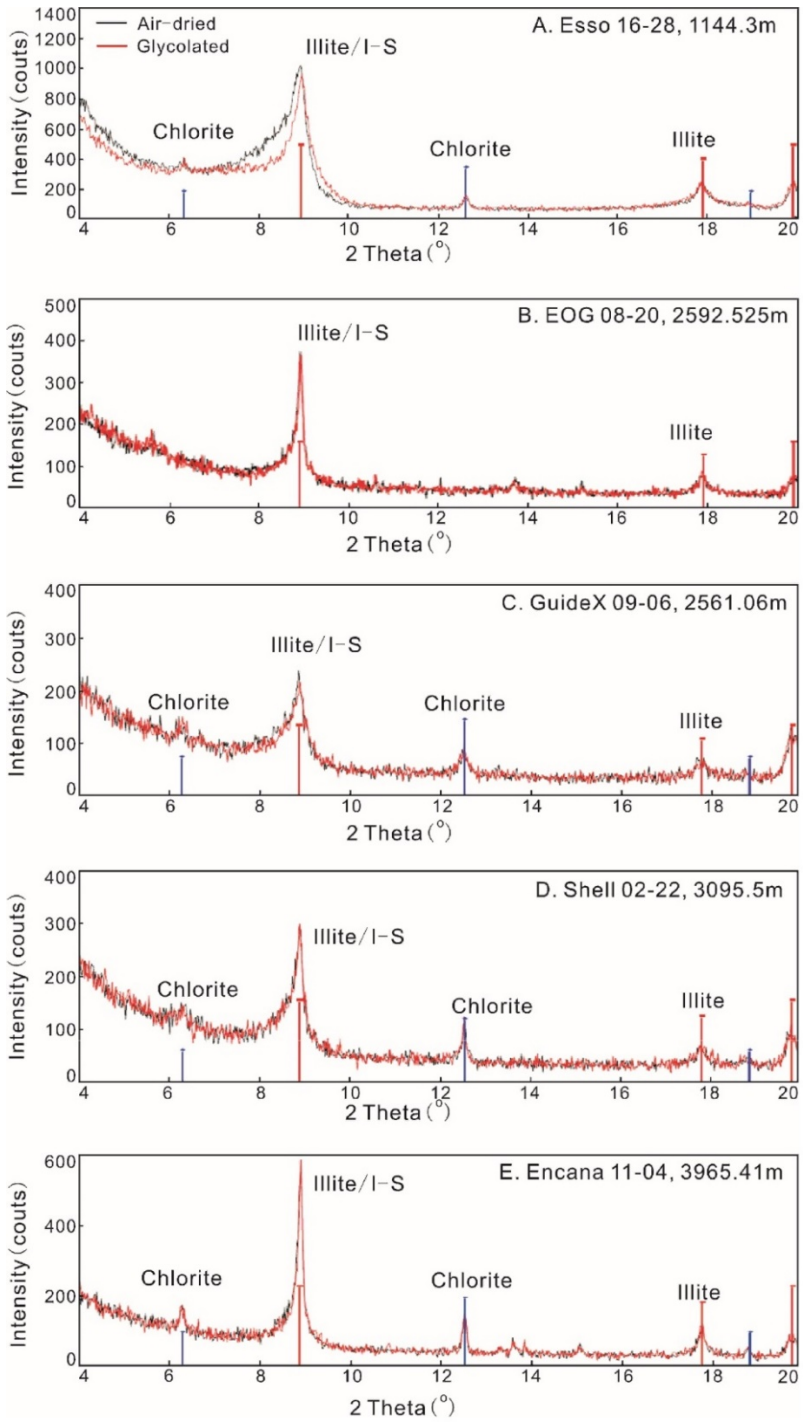

Figure 2. Representative x-ray diffraction analyses of clay separates from Duvernay Formation.

Three distinct models could explain our data: (1) the illite clay was entirely detrital in origin, probably in the form of discrete, finely divided muscovite, and no smecite-rich mixed-layer clay was ever present; (2) original mixed-layer clays had converted to highly illitic clays before burial; or (3) the mixed layer clay conversion took place at relatively shallow burial depths through non-thermally controlled processes. The presence of detrital illite is consistent with a siliciclastic sediment origin from the Canadian Shield and is probably consistent with a northern source as well, although the latter source is more poorly constrained. Illitization of mixed-layer clay in surficial sediment can be driven by alternating seasonal wet-dry cycles (Huggett and Cuadros, 2005), as interpreted for example in mudrocks of the Eocene-Oligocene Solent Group in southern England, which has not been buried deeper than a few hundred meters. The clay assemblage in these sediments consists almost entire of illite and a very illitic mixed-layer clay, similar to observed assemblages in the Duvernay Formation.

Finally, studies of geologically young sediments of the Nankai Trough (Kim et al., 2019) show that microbially induced reduction of Fe (III) in smectite promotes illitization at temperatures much lower than through purely abiotic processes. Van de Kamp (2019) arrived at a similar interpretation for mudrocks in the Ordovician Simpson Group of Oklahoma. The presence of abundant, highly labile Type II organic matter (Harris et al., 2018) suggests that oxidation of shallow methane generated from degradation of organic-rich sediments coupled with reduction of iron in smectite provides a a plausible mechanism for the highly illitic mixed-layer clay assemblage present in the Duvernay Formation. Such a model that would apply to other organic rich mudrocks.

Conclusions

The existence of a low expandability, highly illitic clay mineral assemblage in a low thermal maturity Duvernay mudrock sample and illite clay in remaining samples implies that clay minerals in the Duvernay Formation follow a different pathway than the thermal control clearly described in Tertiary sediments of the Gulf of Mexico. If mixed-layer smectite clays never entered the basin during Duvernay deposition (models 1 and 2, above), the presence of illite or illitic mixed-layer clays reflects provenance rather than thermal maturity; and diagenetic effects such as dissolution of K-feldspar or conversion to albite, authigenic albite, quartz, chlorite and Fe-carbonate cements are unrelated to mixed-layer clay mineral reactions.

Alternatively, biogenically-mediated diagenetic conversation of smectite to illite at shallow burial depth, however, could have produced the observed clay mineral assemblages. In this case, some of the same diagenetic byproducts could have been produced as are associated with the abiotic smectite-to-illite conversion documented in the Tertiary Gulf of Mexico section. In this case, however, the reactions associated with the smectite-to-illite conversion would take place in sediments at shallower burial depths than in the classic models, in rocks that are less compacted – therefore more porous and permeable – and as a result, more open-system behavior could be expected.

Acknowledgements

Analytical work on the Duvernay Formation was funded by Imperial Oil, Shell Canada, ConocoPhillips, Nexen, Devon Energy, and the Natural Sciences and Engineering Research Council of Canada (all on grant number CRD 445064-12).

References

Boles, James R., and Stephen G. Franks. (1979). "Clay diagenesis in Wilcox sandstones of Southwest Texas; implications of smectite diagenesis on sandstone cementation." Journal of Sedimentary Research 49, no. 1, 55-70.

Dong, Tian, Nicholas B. Harris, Levi J. Knapp, Julia M. McMillan, and David L. Bish. (2018). "The effect of thermal maturity on geomechanical properties in shale reservoirs: An example from the Upper Devonian Duvernay Formation, Western Canada Sedimentary Basin." Marine and Petroleum Geology, v. 97, 137-153.

Dong, Tian, Nicholas B. Harris, Julia M. McMillan, Cory E. Twemlow, Brent R. Nassichuk, and David L. Bish. (2019). "A model for porosity evolution in shale reservoirs: An example from the Upper Devonian Duvernay Formation, Western Canada Sedimentary Basin." AAPG Bulletin v. 103, no. 5, 1017-1044.

Freed, Robert L., and Donald R. Peacor. (1989). "Variability in temperature of the smectite/illite reaction in Gulf Coast sediments." Clay Minerals 24, no. 2, 171-180.

Harris, Nicholas B., Julia M. McMillan, Levi J. Knapp, and Maria Mastalerz. (2018). "Organic matter accumulation in the Upper Devonian Duvernay Formation, Western Canada Sedimentary Basin, from sequence stratigraphic analysis and geochemical proxies." Sedimentary Geology 376, 185-203.

Hower, John, Eric V. Eslinger, Mark E. Hower, and Edward A. Perry. (1976). "Mechanism of burial metamorphism of argillaceous sediment: 1. Mineralogical and chemical evidence." Geological Society of America Bulletin v. 87, no. 5, 725-737.

Huggett, J. M., and J. Cuadros. (2005). "Low-temperature illitization of smectite in the late Eocene and early Oligocene of the Isle of Wight (Hampshire basin), UK." American Mineralogist 90, no. 7, 1192-1202.

Jarvie, Daniel M. (2015). “Correlation of Tmax and Measured Vitrinite Reflectance.” http://www.wildcattechnologies.com/application/files/9915/1689/1979/Dan_Jarvie_Correlation_of_Tmax_and_measured_vitrinite_reflectance.pdf.

Kim, Jinwook, Hailiang Dong, Kiho Yang, Hanbeom Park, W. Crawford Elliott, Arthur Spivack, Tae-hee Koo et al. (2019). "Naturally occurring, microbially induced smectite-to-illite reaction." Geology 47, no. 6, 535-539.

Knapp, Levi J., Julia M. McMillan, and Nicholas B. Harris. (2017). "A depositional model for organic-rich Duvernay Formation mudstones." Sedimentary Geology v. 347, 160-182.

Knapp, Levi J., Nicholas B. Harris, and Julia M. McMillan. (2019). "A sequence stratigraphic model for the organic-rich Upper Devonian Duvernay Formation, Alberta, Canada." Sedimentary Geology 387, 152-181.

Land, Lynton S., Larry E. Mack, Kitty L. Milliken, and F. Leo Lynch. (1997). "Burial diagenesis of argillaceous sediment, south Texas Gulf of Mexico sedimentary basin: A reexamination." Geological Society of America Bulletin v. 109, 2-15.

van de Kamp, Peter C. (2019). "Provenance, shallow to deep diagenesis, and chemical mass balance in supermature arenites and pelites, Ordovician Simpson Group, Oklahoma and Kansas, USA." Sedimentary Geology 386, 79-102.

Table 1. Wells included in this study

Well	TOC	Hydrogen index	Oxygen index	Tmax	Production index
Esso Redwater 16-28	avg 2.59% range 0.10 – 9.00%	avg 460 range 159 – 568	avg 52 range 23- 212	avg 422°C range 415 - 432°C	avg 0.08 range 0.03 – 0.44
GuideX Gvillee 09-06	avg 3.34% range 0.56 – 5.54%	avg 337 range 188 – 456	avg 15 range 5 - 59	avg 443°C range 432 - 445°C	avg 0.17 range 0.12 – 0.31
EOG Cygnet 08-20	avg 1.62% range 0.17 – 8.38%	avg 255 range 113 - 458	avg 26 range 3 - 86	avg 448°C range 436 - 454°C	avg 0.33 range 0.02 – 0.57
Shell Kaybob 02-20	avg 2.20% range 0.25 – 5.62%	avg 75 range 42 – 132	avg 13 range 3 - 41	avg 470°C range 443 - 482°C	avg 0.51 range 0.37 – 0.70
Encana Cecilia 11-04	avg 2.40% range 0.28 – 4.88%	avg 33 range 13 – 24	avg 16 range 10 - 19	avg 394°C range 364 - 514°C	avg 0.68 range 0.39 – 0.94

Well name	Depth (m)	Quartz (%)	Plagioclase (%)	K-feldspar (%)	Calcite (%)	Dolomite (%)	Ankerite (%)	Pyrite (%)	Mica (%)	Clay (%
East Shale Basin										
Esso 16-28	1121.48	11.5	1.9	3.4	71.5	0.5	0	1	2	7.1
Esso 16-28	1144.3	10.2	0	5.2	70	0	1.9	1.5	1.1	9.7
Esso 16-28	1157.49	17.8	0	12.2	44	0	4	2.4	6.1	13.3
EOG 08-20	2574.515	3.9	0	0	92.6	0	0.5	0	0.1	2.3
EOG 08-20	2592.525	11.1	0	13.7	59.8	0	0	1.7	3.7	9.6
West Shale Basin										
GuideX 09-06	2558.2	12.7	0.5	0	86.1	0	0	0.5	0	0
GuideX 09-06	2558.71	35.2	1.3	4.4	4.8	1.2	0	1.5	14.9	36.7
GuideX 09-06	2561.06	24.5	2.7	3.3	27.8	25	0.6	1.4	2.2	12.5
Shell 02-22	3095.5	37.9	1.9	5.8	20.4	0.9	1.3	2.6	4.9	24.3
Shell 02-22	3112.5	44	0.7	11.9	16.2	0	0	1.4	5.9	19.7
Encana 11-04	3956.475	22.5	2.1	11.6	12.6	0	5	1.2	10.3	34.9
Encana 11-04	3965.41	28	2.7	17.4	25.4	0.5	0	1.8	5.1	19.1
Encana 11-04	3985.465	23.3	1.6	6.5	59.8	0.6	0	1.3	2.2	4.8